



Original Research

Experimental study on the effect of bottomless structure in front of a bottom outlet on a sediment flushing cone

Hadi Haghjoei^a, Majid Rahimpour^{a,*}, Kouros Qaderi^a, Sameh A. Kantoush^b^a Department of Water Engineering, Shahid Bahonar University of Kerman, Kerman, Iran^b Disaster Prevention Research Institute, Kyoto University, Japan

ARTICLE INFO

Article history:

Received 5 September 2019

Received in revised form

6 November 2020

Accepted 9 November 2020

Available online 16 November 2020

Keywords:

Reservoir

Sediment removal efficiency

Sediment flushing cone

Bottom outlet

Dendritic bottomless extended structure

ABSTRACT

One of the main problems in reservoirs is sedimentation which reduces the operating life of dams if a proper plan and analysis method are not in place. The techniques to manage sediment in reservoirs include several sustainable management techniques that route sediment through or around the reservoir. One of the main economical methods in arid and semi-arid regions is pressurized flushing using moderate drawdown of the water level of the reservoir to evacuate sediment deposited behind dams. In the current study, the effect of a new structure called a dendritic bottomless extended (DBE) outlet structure at three angles of 30°, 45°, and 60° on pressurized flushing efficiency was investigated. Consequently, 45 experiments were designed for three discharge rates (Q_0), three sediment levels (H_s), four types of structure, and a no-structure condition (reference test). The results indicated that the DBE structure with a 30° angle between the branches, a sedimentary dimensionless index of $H_s/D_0 = 4.59$, and a flow dimensionless index of $Q_0/\sqrt{gD_0^5} = 1.43$ (where g is the acceleration of gravity and D_0 is the diameter of the bottom outlet) lead to 10-fold increase in the sediment flushing cone dimensions and sediment removal efficiency compared to the results of the reference test. Finally, according to a statistical analysis of the results, a dimensionless equation for calculating the sediment flushing cone dimensions was developed for the tested sediment characteristics.

© 2020 International Research and Training Centre on Erosion and Sedimentation/the World Association for Sedimentation and Erosion Research. Published by Elsevier B.V. All rights reserved.

1. Introduction

Sedimentation in a reservoir gradually decreases the water storage capacity and can eventually decrease electricity production (White, 2001). The annual rate of water storage capacity reduction due to reservoir sedimentation is faster than new storage due to building new reservoirs and it threatens the lives of existing reservoirs (Randle et al., 2019; Schleiss et al., 2016). In addition, sedimentation has other negative consequences such as the entry of sediment to hydropower plant intakes which leads into hydro-abrasive erosion in turbines (Dreyer & Basson, 2018), intake obstruction, increases in the reservoir upstream level, and expansion of the flood width (Morris & Fan, 1998). A low-level outlet is one of the important components of dams and can be used to expel the flood discharge and sediment. The use of these outlets is only

recommended in cases with a low degree of risk because sediment and debris can clog low-level outlets (Amirsayafi, 2015).

Minimizing the loss of storage capacity is one of the main purposes of sustainable management of sedimentation and there are several management strategies depending on infrastructure purposes, storage lost, and sedimentation rate (Schleiss et al., 2016). Sediment management strategies can be categorized in three groups depending on their location upstream of the reservoir, in the reservoir, and at the dam, such as decreased sedimentation via watershed management, e.g., via upstream check dams; managing sediment within the reservoirs through dams, e.g., dredging of accumulated sediment; and sediment removal in reservoirs, e.g., hydraulic flushing and sluicing (Annandale et al., 2016; Schleiss et al., 2016).

Hydraulic flushing is a method in which the low-level outlet is opened and old deposited sediment evacuates the reservoir through the flow. It is an effective solution for reservoirs with excessive water inflows (Qian, 1982). Flushing can be used to evacuate sediment and improve the useful capacity of the reservoir.

* Corresponding author.

E-mail address: Rahimpour@uk.ac.ir (M. Rahimpour).

This process also can be used for both small and large reservoirs (Emamgholizadeh et al., 2006). Sediment flushing can be categorized into two types of drawdown flushing (also known as free-surface, empty, or free-flow flushing) and pressurized flushing (Morris & Fan, 1998). Free flow or drawdown flushing is done by lowering the water level of reservoirs and it is commonly practical in small and medium reservoirs (Isaac & Eldho, 2019). Pressurized flushing is done with a moderate drawdown for effective operation, but the drawdown flushing requires a high drawdown and the water level reaches the level of the low-level outlet (Dargahi, 2012).

In the pressurized flushing method, the water height is higher than the low-level outlet and after opening the low-level outlet, the outlet-induced-vortex creates a shear force on the deposited sediment and sediment evacuates the reservoir. In this method, after a while, a hollow or scour hole forms in the shape of a cone or funnel in front of the bottom outlet. The duration of the complete formation of the scour hole and the equilibrium of its geometrical dimensions depend on the type of sediment, the reservoir water level, and the height of the accumulated sediment above the low-level outlet and the duration may range from several hours to several days (Brandt & Swening, 2000). Drawdown flushing leads to high sediment loads with a low water value that can threaten life in downstream watercourses (e.g., fish mortality) and water quality (Malavoi & El Kadi Abderrezzak, 2019). Climate conditions can be restrictive in the choice of sediment management strategies. For example, drawdown flushing is not an option in arid and semi-arid conditions (Schleiss et al., 2016).

One of the main disadvantages of pressurized flushing is the low ability to recover a large amount of storage capacity because of the localized effects near the bottom outlet. But pressurized flushing keeps the power intake free of sediment and the water loss is much less compared to drawdown flushing, making this method of flushing more practical for hydropower dams in arid and semi-arid countries (Dreyer, 2018). For reservoirs with supply storage ratios of less than 0.5 in relation to the inlet flow, hydraulic flushing is a good method to maintain the reservoir storage capacity (Pitt & Thompson, 1984). In addition, flushing can also be successfully utilized in irrigation and hydropower plant reservoirs that operate on monthly to daily periods. Flushing can also be used in reservoirs that are hydrologically large but have reduced storage capacity due to sediment accumulation. The range of sediment that is removed from the reservoir due to flushing varies from sand to clay in particle size (Morris & Fan, 1998). Flushing is a necessary action to keep the reservoir in the best operating condition (Fruchard & Camenen, 2012).

Many investigations, consisting of experimental scale and numerical simulation models, have been done on the sediment flushing characteristics. Application of one-, two-, and three-dimensional numerical models is common to simulate sediment flushing and reservoir sedimentation. 1D numerical models are used to investigate the reservoir sedimentation, and 2D and 3D numerical models are used to investigate the sediment flushing from reservoirs (Isaac & Eldho, 2019). Di Silvio (1990) experimentally investigated low-level outlet blockage and observed that to avoid blockage, the initial and final phases of sediment flushing should be considered. Powell (2007) investigated the effect of the sediment size and water depth on the sediment flushing cone dimensions and found a complex vortex system governing the equilibrium size of the sediment flushing cone. Emamgholizadeh et al. (2006) investigated the effect of the water height on the

low-level outlet and outlet discharge on the sediment flushing cone. The results of their study showed that when the height of the water decreases, the length and volume of the sediment flushing cone increases and when the discharge from the low-level outlet is reduced, the length and volume of the sediment flushing cone decrease. Meshkati et al. (2009) experimentally investigated the temporal development of sediment flushing cones. They observed that with an increase in the flow velocity, sudden increases in the amount of evacuated sediment and the dimensions of the sediment flushing cone were created. In addition the same authors (Meshkati et al., 2010) experimentally investigated the effect of the cross section of the low-level outlet on the dimensions of the sediment flushing cone. They concluded that the volume and dimensions of the sediment flushing cone heavily depend on the low-level outlet diameter.

Ahadpour Dodaran et al. (2012) experimentally investigated the effect of local vibrations on sediment flushing cone dimensions and determined the optimal vibrator distance from the outlet. The effect of the geometric parameters and the discharge of a perpendicular water jet with four jet arranged in a horizontal plane was investigated by Jenzer Althaus et al. (2014). Their results showed that using a water jet as an innovative device which can whirl up the sediment, leads to between a 1.5- and 2-fold increase in sediment evacuation efficiency compared to the results of the reference case.

An experimental study was done by Emamgholizadeh and Fathi-Moghadam (2014) to investigate the effects of flow parameters on the sediment flushing cone formation of five classes of sediment samples from the Dez Dam Reservoir in Iran and they found that the bulk density of the sediment samples is the most significant parameter related to the sediment flushing cone dimension. Sayah (2015) designed the Cerro del Aguila Dam and investigated the elevation of the bottom outlet to avoid plugging in the sediment-flushing process. They recommended that the low-level outlet gates be designed with a sufficient size to avoid blockage. Amirsayafi (2015) investigated measures for the successful design of dam-bottom outlets and found that for the effective operation of dams, low-level outlets should not be blocked by sediment and debris. Madadi et al. (2016) did tests in two parts in an experimental study to investigate: 1) the flow behavior during the formation of a sediment flushing cone, and 2) the effect of semi-confined piles on the sediment flushing cone. Their results showed that the interactions among sediment, water, and the structure led to an increase in the sediment flushing cone dimensions. In another study by the same authors (Madadi et al., 2017), the effect of a projecting semi-circular (PSC) structure on the sediment flushing cone was investigated. They found that using the PSC structure led to a 4.5-fold increase in the sediment flushing cone volume compared to that in the reference test. Considering the effect of the PSC structure in the experimental study by Madadi et al. (2017) attention to the sediment flushing operation of the PSC structure on the direct side of the reservoir is necessary to avoid blocking of the low-level outlet.

The aim of this study was to investigate the structural effects on the sediment flushing cone dimensions and efficiency due to vortices arising from the pressure difference between the inside and outside of the structure and the flow area limitation of the structure's branches. Consequently a new structural configuration with the ability of flushing at different sides of the reservoir in addition to the direct path which called dendritic bottomless

extended structure (DBE) at three angles of 30°, 45°, and 60° on a sediment flushing cone, was used to evacuate the sediments in the blockage and no blockage position. Considering the installation of branches at specific points, in addition to generating a vortex along any of the branches, increasing the strength of the vortices will increase the outflow, and the dimensions of the cone.

2. Materials and methods

2.1. Description of the physical model

To investigate the effect of the structures and the rate of pressurized sediment flushing on sediment removal, a physical and hydraulic model of a dam and water conduit was designed and constructed in the Hydraulic and Water Structures Research Laboratory of the Water Engineering Department of Shahid Bahonar University of Kerman, Iran. The current model is composed of a rectangular cube with dimensions of 7.5 m × 3.5 m × 1.8 m in length, width, and height, respectively. The model consists of 5 major segments: 1) an area consisting of perforated cover plates for dissipating the inlet flow, 2) a reservoir, 3) a sediment-trapping box,

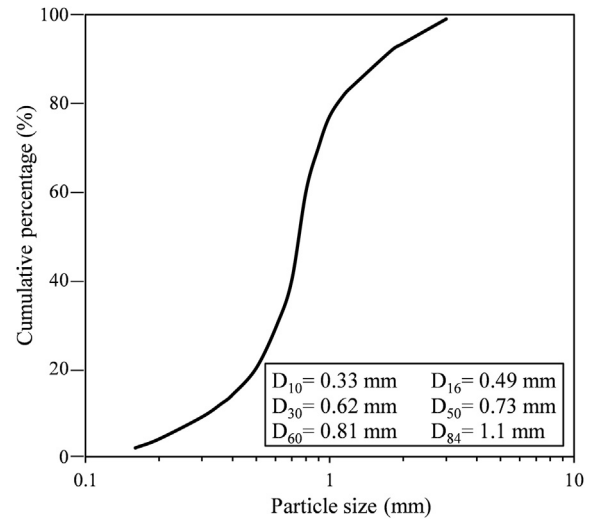


Fig. 2. Particle size distribution curve of bed sediment (where D_x is the sediment diameter for which x percent of the sediment particles are finer).

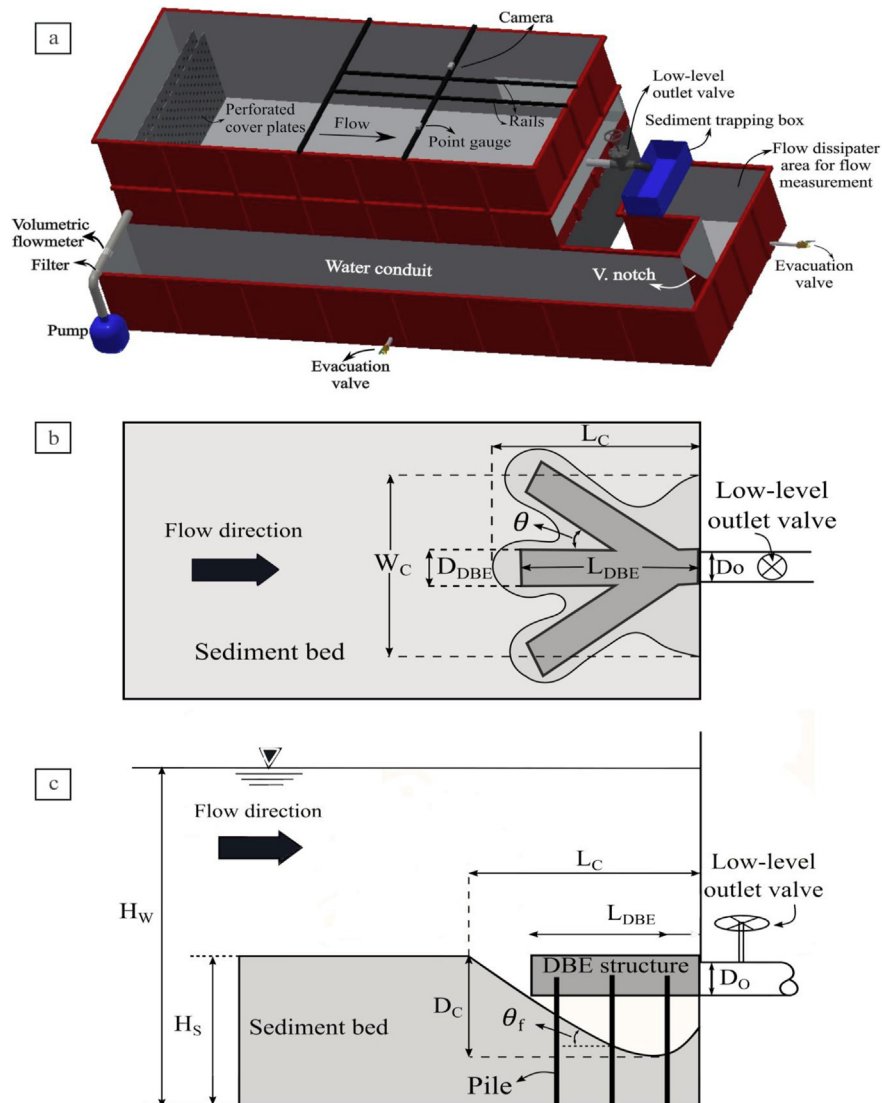
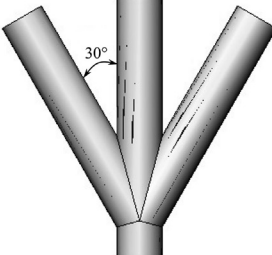
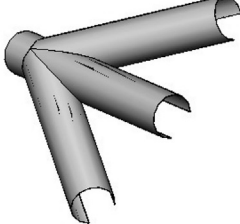
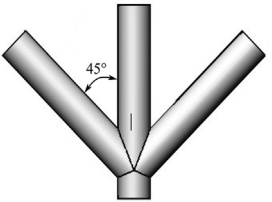
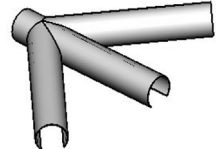
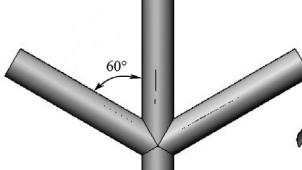
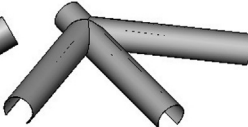




Fig. 1. 3D schematic representation of the physical model, perspective, plan, and side view (a, b, and c, respectively).

Table 1
Experiments done in the current research.

Test no.	Name	Q_0 (L/s)	H_s (cm)	Schematic configuration of structures
1	a _{1,1}	12.5	39.5	 <p>DBE 30°</p> 
2	b _{1,1}			
3	c _{1,1}			
4	d _{1,1}			
5	e _{1,1}			
6	a _{2,1}	15		
7	b _{2,1}			
8	c _{2,1}			
9	d _{2,1}			
10	e _{2,1}			
11	a _{3,1}	18		 <p>DBE 45°</p> 
12	b _{3,1}			
13	c _{3,1}			
14	d _{3,1}			
15	e _{3,1}			
16	a _{1,2}	12.5	45	
17	b _{1,2}			
18	c _{1,2}			
19	d _{1,2}			
20	e _{1,2}			
21	a _{2,2}	15		 <p>DBE 60°</p> 
22	b _{2,2}			
23	c _{2,2}			
24	d _{2,2}			
25	e _{2,2}			
26	a _{3,2}	18		
27	b _{3,2}			
28	c _{3,2}			
29	d _{3,2}			
30	e _{3,2}			
31	a _{1,3}	12.5	50.5	 <p>PSC</p> 
32	b _{1,3}			
33	c _{1,3}			
34	d _{1,3}			
35	e _{1,3}			
36	a _{2,3}	15		
37	b _{2,3}			
38	c _{2,3}			
39	d _{2,3}			
40	e _{2,3}			
41	a _{3,3}	18		
42	b _{3,3}			
43	c _{3,3}			
44	d _{3,3}			
45	e _{3,3}			

Note: $x_{i,j}$, where x = type of structures, consisting of a, b, c, d, and e where a = DBE 30°, b = DBE 45°, c = DBE 60°, d = PSC structure, and e = reference test (no-structure); and i,j = indexes of discharge and sediment height for which $i = 1, 2,$ and 3 are discharges of 12.5, 15, and 18 L/s, respectively; and $j = 1, 2,$ and 3 are sediment heights of 39.5, 45, and 50.5 cm, respectively.

4) a flow dissipater area for flow measurements, and 5) a water conduit. A schematic view is shown in Fig. 1.

At a distance of 50 cm from the beginning of the reservoir, there are two perforated cover plates for reducing the turbulence of the inlet flow to the reservoir. A laminated glass was used in the front and side of the model to accurately observe the flow and sediment behavior through the experiments. In the front part, a hole was made with a diameter of 12 cm, through which the outlet pipe of the reservoir passes with a diameter (D_0) of 11 cm. A bottomless pipe,

with a horseshoe cross section with a 47° angle between the sediment bed surface and tangent line to the pipe at the intersection point, is connected to the upstream edge of the bottom outlet. A volumetric flow meter and a triangular weir with a 90° angle were used to measure the inlet and outlet flow, respectively. After passing through the outlet pipe, the sediment flow first enters the sediment-trapping box and then flows into the flow dissipater area to measure the outlet discharge. In each experiment, the weight of the deposited sediment was measured in the sediment-trapping area after drying.

In the current study, a non-cohesive silica sediment with a median diameter of $D_{50} = 0.73$ mm and a specific gravity of 2.625 was used (Fig. 2). The corresponding internal friction angle of this sediment was 29° .

The experiments were done for three discharges (Q_o) of 12.5, 15, and 18 L/s; three sediment levels (H_s) of 39.5 cm (no blockage), 45 cm (blockage height = $D_o/2$), and 50.5 cm (blockage height = D_o) from the reservoir bed; four structural conditions consisting of dendritic modes at three angles (θ) of 30° , 45° , and 60° between the branches, a PSC structure, and a no-structure mode as the reference test. The water level for all the tests was constant and equal to 65 cm. Therefore, the total number of experiments was 45 and the experimental characteristics are listed in Table 1.

2.2. Test procedure

Before doing each test, sediment was poured into layers, and using a prismatic straightener, the surface of the sediment was leveled according to the rulers installed in the reservoir. In the current study, three sediment levels were used: a) the lower edge of the low-level outlet (without blockage), b) a blockage equal to half of the outlet diameter, and c) a blockage of the entire outlet diameter (Fig. 3).

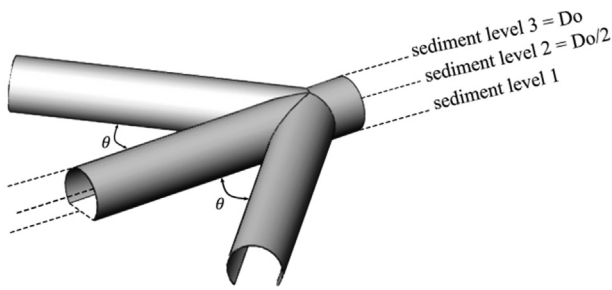


Fig. 3. Schematic configuration of sediment levels and structure settlement.

To prevent the degradation of the sediment surface, at the beginning of each test, a low-rate foam pump was used. After the reservoir water level reached the desired level, the centrifugal pump turns on and the low-level outlet valve opened. The water level was measured by a manual pointer gauge with a precision of ± 1 mm and rulers mounted on the sides of the reservoir. To obtain the topography of the sediment cone in each experiment, a photo scanning technique (PST) was used. Following the completion of each test and ensuring full drainage of the main reservoir, photographs were recorded with the given horizontal and vertical spacing (three horizontal rows and four vertical rows) on camera rails, and an advanced Canon IXUS 190 with remote control ability also was utilized. Then, the photos were analyzed and the output of xyz points was imported into ArcGIS as a dense-point cloud to measure the volume. To draw the profiles, Surfer 16 was utilized. The PST primary was investigated and calibrated on a cube with known dimensions and volume. According to the measuring distance, the typical data accuracy was determined to be 1.4 mm at a distance of 40 cm. The results were compared with the data accuracy of a DPI-8 handheld scanner in Dreyer (2018) and are listed in Table 2.

In the current study, the volume of the sediment flushing cone was measured using the PST based on the difference between the level surface of the sediment before the insertion of the structure and the situation after the removal of the structure and completion of the test (Fig. 4).

2.3. DBE structure

Increasing the sediment removal efficiency is very important, but, according to the previous literature, the aim of most studies has been to recognize the mechanism of flushing and the effect of hydraulic parameters on the sediment flushing cone dimensions. Madadi et al. (2017) utilized a new configuration of the dam bottom outlet, a PSC structure, to increase the efficiency of sediment evacuation. In the current research a new structure configuration involving a dendritic bottomless extended low-level outlet structure (DBE structures), was developed and used for the sediment flushing of reservoirs. As shown in Fig. 5, the DBE structure is connected to the dam body on one hand and is connected to the bed reservoir with piles from the other hand. In addition, the DBE structure has the ability to flush sediment from three sides and avoid sediment blockage in low-level outlets. Based on the circular cross section of the DBE structure the probability of instability of the structure is negligible. Similar to the PSC structure, because of the circular shape of the structure, not only the concentration stresses are on the crown of the structure, but also the vertical forces are transferred to the reservoir bed through the piles (Madadi et al., 2017). One of the greatest advantages is the existence of the structure's branches in different aspects of the reservoir leads to an increase in the sediment removal domain. In this structure, similar to the PSC structures, the water flow contacts the interior parts of the reservoir floor. The DBE structures are designed and made 800 mm in length and 160 mm in diameter, and with angles of 30° , 45° , and 60° between the branches. The structures are linked to the bottom outlet from one side and through the metal bases to the deposited sediment in the reservoir (Fig. 5).

2.4. Dimensional analysis

The sediment flushing cone volume (V_c) depends on main variables such as the fluid dynamic viscosity (μ), outflow discharge (Q_o), total water head above the bottom-outlet (H_w), the sediment head above the bottom-outlet (H_s), the median size of sediment (D_{50}), the sediment density (ρ_s), the internal friction angle of the sediment (θ_f), the fluid density (ρ_w), the acceleration due to gravity (g), diameter of the bottom-outlet (D_o), diameter of DBE structure (D_{DBE}), length of the branches of the DBE structure (L_{DBE}), angle between the branches of the DBE structure (θ), and the number of branches of the DBE structure (N) as follows:

$$V_c = f(Q_o, H_w, H_s, D_{50}, \rho_w, \rho_s, \theta_f, \mu, g, D_o, D_{DBE}, L_{DBE}, \theta, N) \quad (1)$$

The resulting terms of the dimensional analysis are obtained as follows:

$$\frac{V_c}{D_o^3} = f_1 \left(\frac{Q_o}{\sqrt{g D_o^5}}, \frac{H_w}{D_o}, \frac{H_s}{D_o}, \frac{D_{50}}{D_o}, \frac{\rho_s}{\rho_w}, \theta_f, \frac{4\rho Q_o}{\mu\pi D_o}, \frac{D_{DBE}}{D_o}, \frac{L_{DBE}}{D_o}, \theta, N \right) \quad (2)$$

On the other hand, the following equation is obtained:

$$\frac{V_c}{D_o^3} = f_2 \left(\frac{Q_o}{\sqrt{g D_o^5}}, \frac{H_w}{D_o}, \frac{H_s}{D_o}, \frac{D_{50}}{D_o}, G_s, \theta_f, Re, \frac{D_{DBE}}{D_o}, \frac{L_{DBE}}{D_o}, \theta, N \right) \quad (3)$$

where G_s = specific gravity of the sediment, and Re = the Reynolds number.

In all the tests, the sediment specific gravity (G_s) was constant because the same sediment material was used in all tests. The

Table 2
Data accuracy of the PST and compression with a DPI-8 handheld scanner.

Range (m)	DPI-8 handheld scanner		PST	
	Typical accuracy (RMSE)	Minimum accuracy	Typical accuracy (RMSE)	Minimum accuracy
<1	0.2%	0.5%	0.26%	0.512%
1–2	0.5%	0.8%	0.31%	0.58%

Note: RMSE = root mean square error.

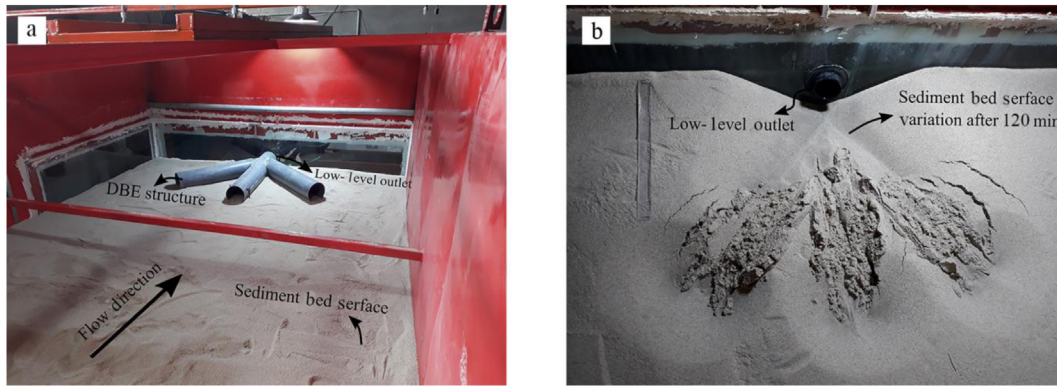


Fig. 4. Situation of sediment bed and structure: $t_1 = 0$ (a) and $t_2 = 120$ min (b).

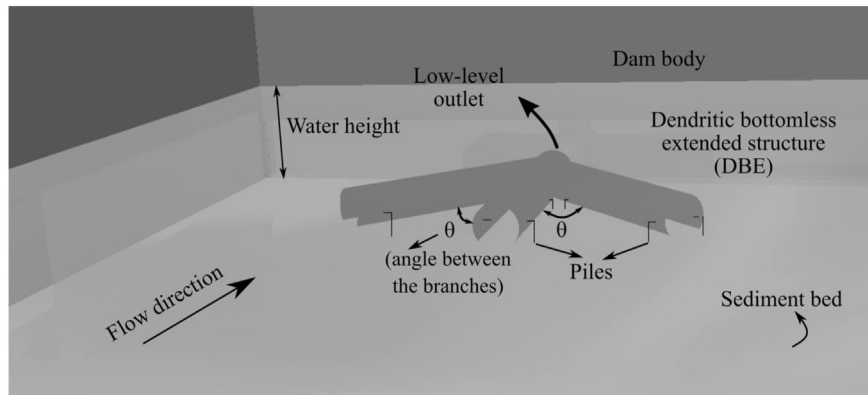


Fig. 5. Schematic representation of DBE structure at $\theta = 30^\circ, 45^\circ,$ and 60° , connected to upstream side of the dam body.

Reynolds number ($\frac{4\rho Q_0}{\mu\pi D_0}$) was considered negligible under a fully turbulent flow from the orifice (Madadi et al., 2017). One sediment characteristic was tested, and thus, the effect of the internal friction angle of the sediments (θ_f), has been neglected and the findings are applicable for the type of sediment tested. In addition, $D_{50}, D_o, H_w, \theta_f, D_{DBE}, L_{DBE}$, and N were constant in this experimental research, and, therefore, $\frac{H_w}{D_o}, \frac{D_{50}}{D_o}, \theta_f, \frac{D_{DBE}}{D_o}, \frac{L_{DBE}}{D_o}$, and N remained constant. The minimum value of particle Reynolds number was 143.35 and this is greater than the minimum value of 70 for creating hydraulic fully rough bed (Shahirmia et al., 2014). The constant values are listed in Table 3.

Regarding the foregoing explanations, Eq. (3) can be simplified as follows:

$$\frac{v_c}{D_o^3} = f_3 \left(\frac{H_s}{D_o}, \frac{Q_o}{\sqrt{g} D_o^5}, \theta \right) \tag{4}$$

According to Eq. (4), to determine the optimal dimensions, the dimensionless variation of $H_s, Q_o,$ and θ are investigated in the current research. Also the other important calculated parameters in the current research are listed in Table 4.

3. Results and discussion

In the design of the experiments in addition to the DBE structures at three angles of $30^\circ, 45^\circ,$ and 60° , the PSC structure and a

Table 3
The constant values in the current research.

$\frac{H_w}{D_o}$ (dimensionless)	$\frac{D_{50}}{D_o}$ (dimensionless)	$\frac{D_{DBE}}{D_o}$ (dimensionless)	$\frac{L_{DBE}}{D_o}$ (dimensionless)	N (dimensionless)	θ_f (degree)	G_s (dimensionless)
5.909	0.00664	1.454	7.273	3	29	2.625

Table 4
The other important calculated values in the current research.

Froude number (bottom outlet)	Reynolds number (bottom outlet)		Reynolds number (sediment particle)		Critical value of Shields parameter	Critical value of shear stress
	Minimum	Maximum	Minimum	Maximum		
4.909	144,686	208,348	143.35	392.744	0.03	0.349

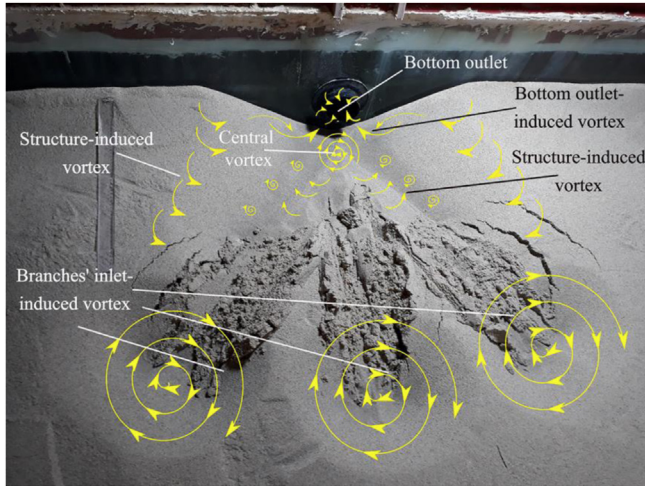


Fig. 6. Flow pattern upstream of the outlet, $a_{3,3}$ configuration (Table 1).

reference test (without a structure) were utilized. The common point of all the experiments was that in a time interval of 15–20 min, a large amount of sediment was excavated from the low-level outlet via the flushing operations, which conformed with the results of Madadi et al. (2016). At the beginning of the experiment, a volume of sediment is discharged due to the opening of the

valve and formation of high-turbulence and high-velocity in the discharge flow from the reservoir. The next step is the simultaneous effect of the vortices and the flow from the outlet. These vortices at the bottom and the two sides of the outlet through the alternating operation cause the sediment to vacate (Fig. 6).

The major difference between the DBE and PSC structures is in the sediment flushing cone shape, the cone for the DBE is wider and deeper than that of the PSC. The reason for this difference is the motion of the current through the branches to a focused point near the outlet, which creates a strong vortex, especially beneath the outlet. In addition, due to the difference in pressure inside and outside of the structure, the erosion is of the type of piping on both sides and along the length of the structure (Madadi et al., 2017).

3.1. Investigation of the geometry of the sediment flushing cone

After each experiment, in addition to taking photos and analyzing the PST at different points, the length, width, and depth of the sediment flushing cone (L_c , W_c , and D_c , respectively) also were measured. Measurements were based on different states of variation in the sediment height and flow discharge, and three graphs related to the changes in L_c , W_c , and D_c also were prepared.

Fig. 7 shows the effects of the dimensionless index of discharge changes in the four states of the structure and the reference test. As shown, with the increase in the dimensionless index of flow from 0.99 to 1.43, the length of the maximum increase in the sediment flushing cone becomes 4.92 times the reference value, the

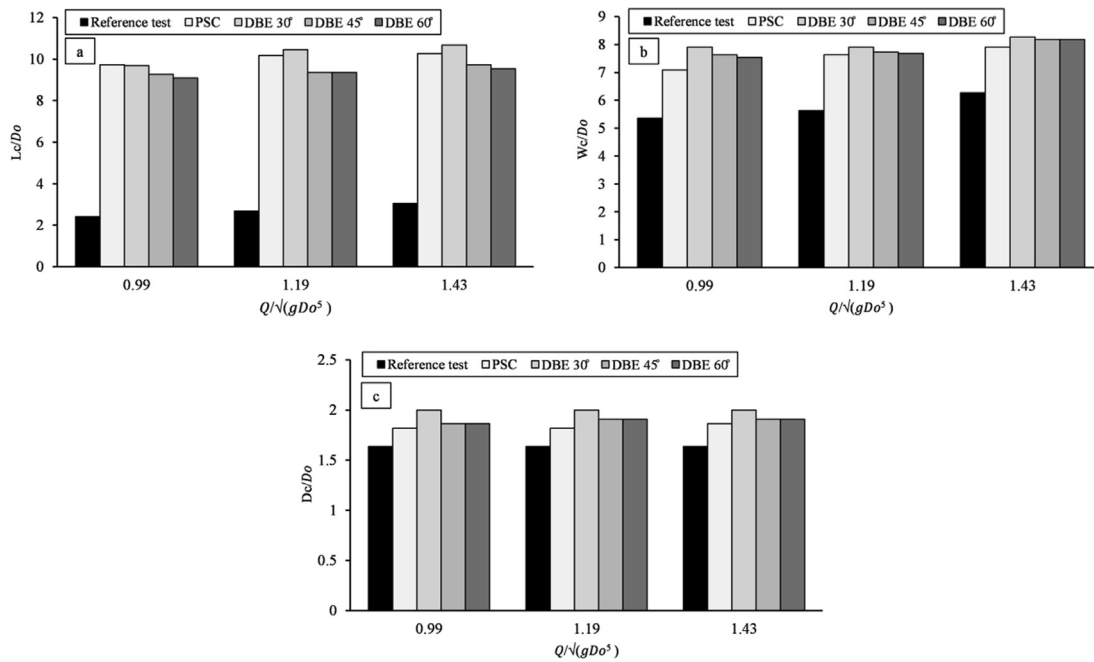


Fig. 7. Variation in the sediment flushing cone dimensionless length (L_c/D_o) (a), width (W_c/D_o) (b), and depth (D_c/D_o) (c), respectively, with dimensionless index changes in discharge ($Q/(gD_o^3)$) in the full blockage state (sediment height = 50.5 cm).

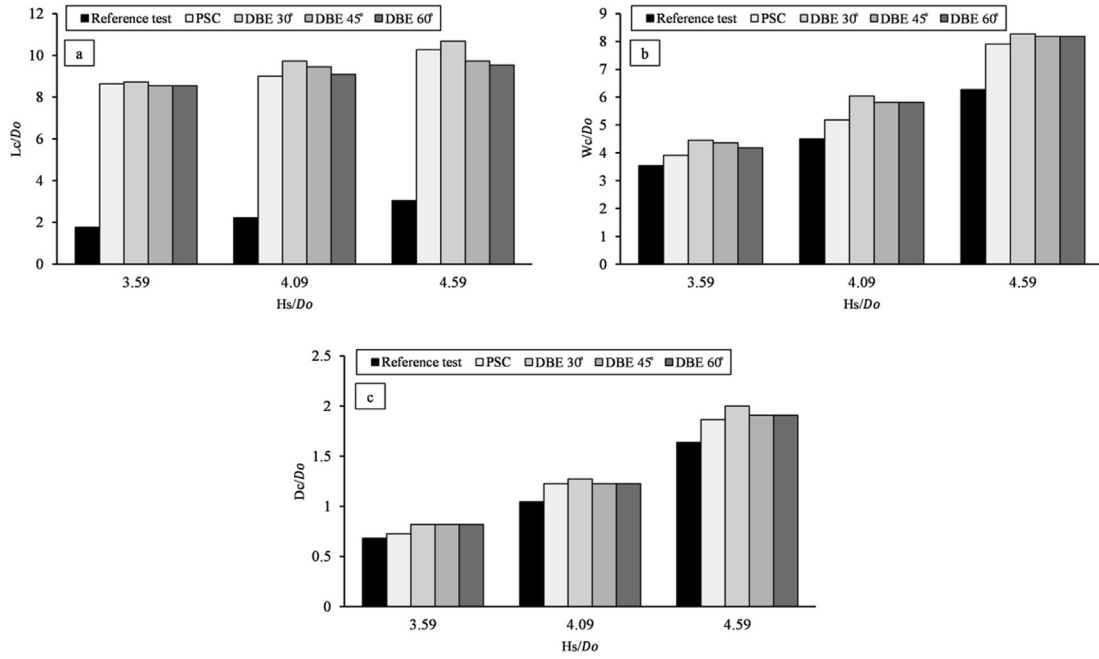


Fig. 8. Variation in the sediment flushing cone dimensionless length (L_c/D_o) (a), width (W_c/D_o) (b), and depth (D_c/D_o) (c), respectively, with dimensionless index changes in the sediment height (H_s/D_o) for discharge = 18 L/s.

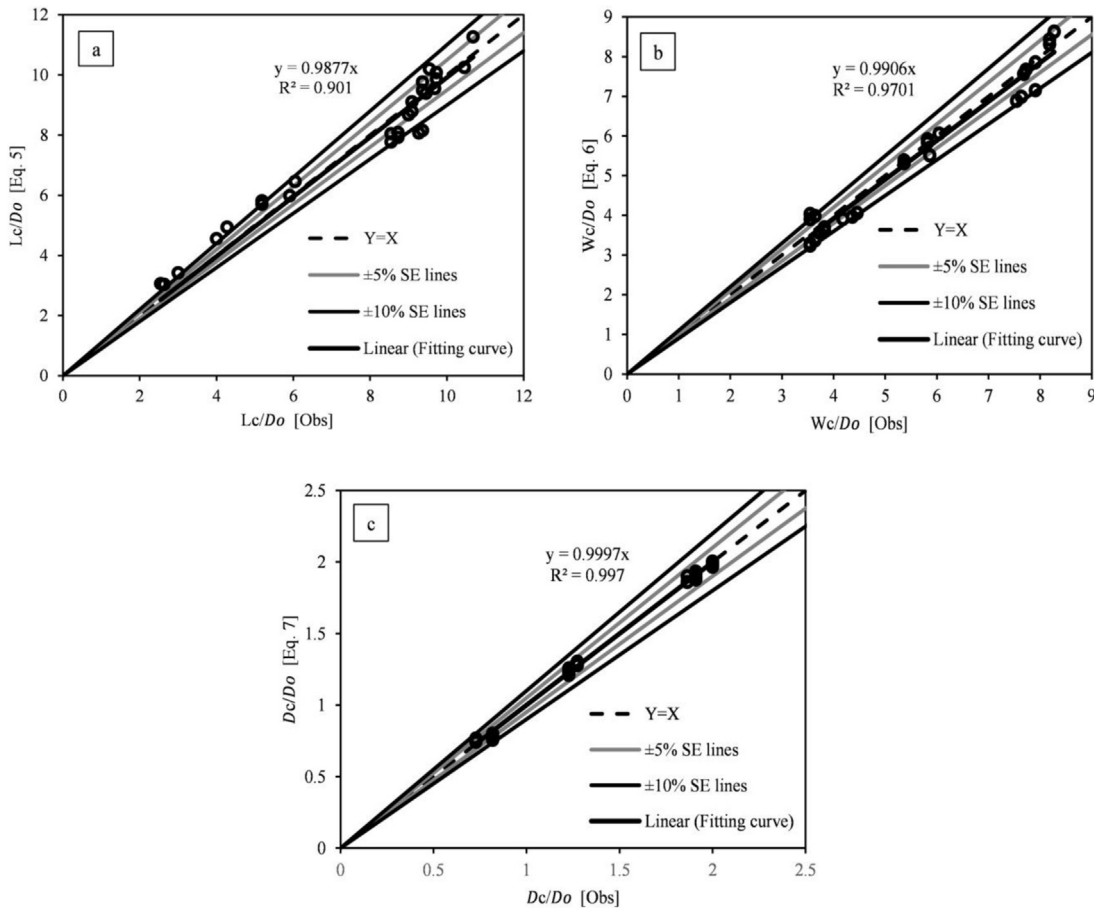


Fig. 9. Observed vs. calculated sediment flushing cone length (L_c/D_o), width (W_c/D_o), and depth (D_c/D_o) dimensionless indexes (a, b, and c, respectively). (Note: SE lines are the standard error lines representing the average distance the observed values fall from the regression line, Linear (fitting curve) is regression line indicating the agreement rate between the observed and calculated values, and R^2 is the coefficient of determination of the prediction equations).

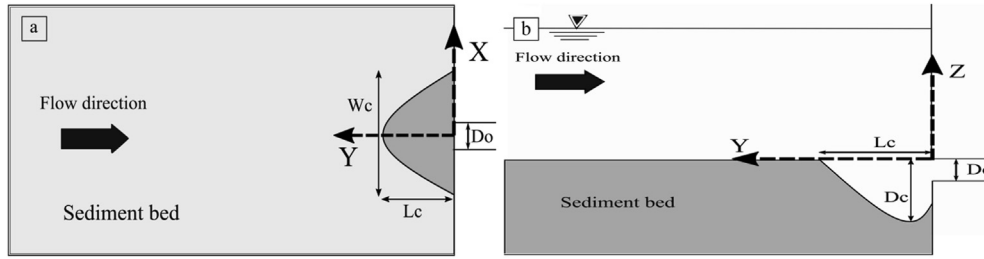


Fig. 10. Coordinate system of the experimental setup: top view (a) and side view (b).

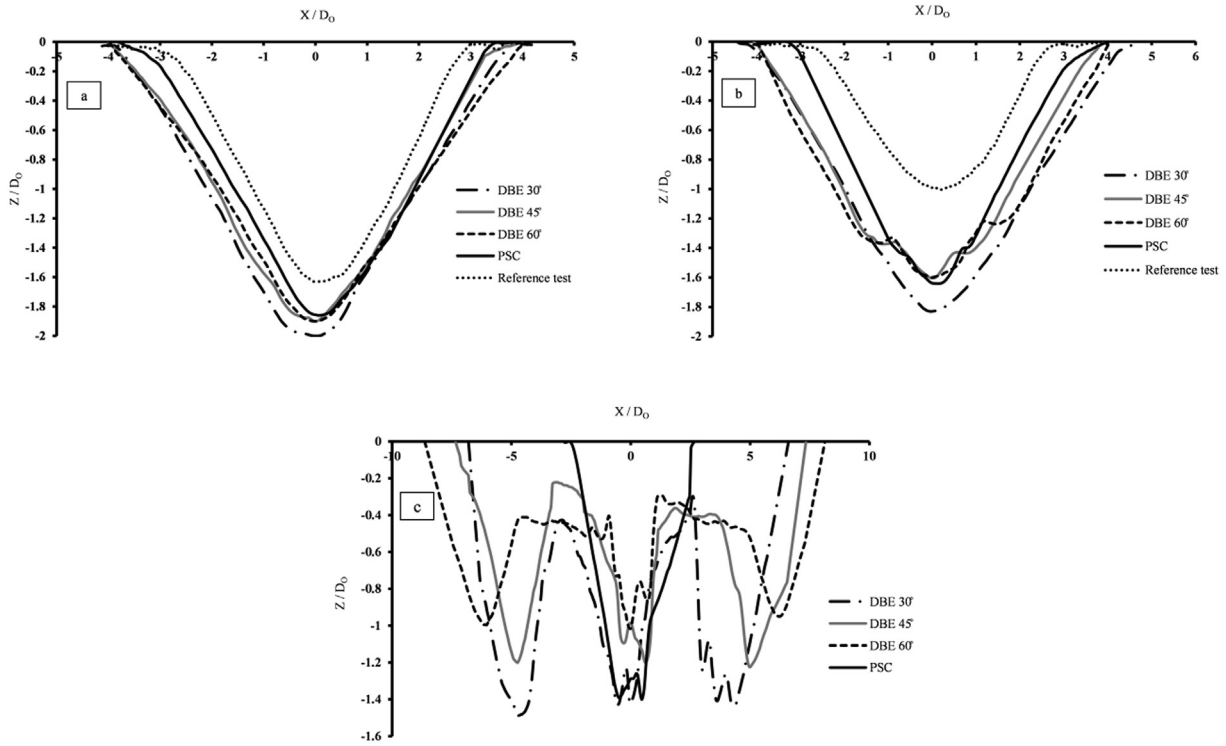


Fig. 11. Transverse cross section of the sediment flushing cone in tests $a_{3,3}$, $b_{3,3}$, $c_{3,3}$, $d_{3,3}$, and $e_{3,3}$ for three different distances of $Y/D_o = 0.5$ (a), $Y/D_o = 1$ (b), and $Y/D_o = 6.36$ (c) from the outlet.

maximum increase in the width of the sediment flushing cone is equal to 1.34 times the reference value, and the depth of the cone with a constant increase is equal to 1.21 times the value in the reference test for three levels of blockage, these findings are identical to the results of Madadi et al. (2017).

Fig. 8 shows the effects of the dimensionless index of the sediment height changes in the four states of the structure and the reference test. As presented, with the increase in the dimensionless index of the sediment height from 3.59 to 4.59, the length of the maximum increase in the sediment flushing cone becomes 4 times

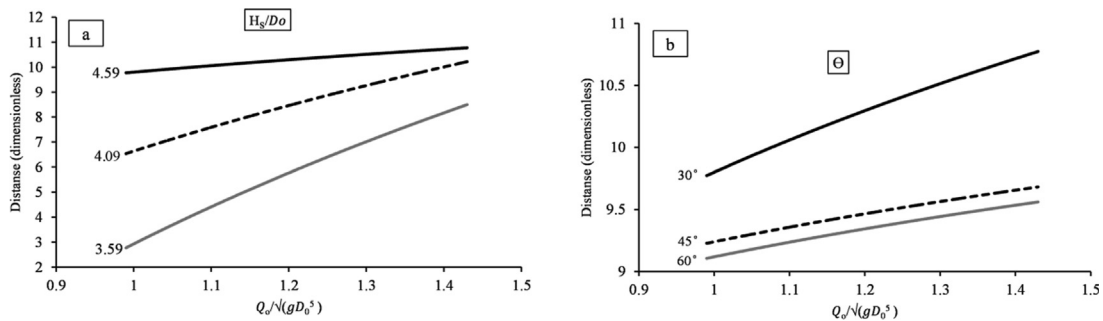


Fig. 12. Scour limit vs. discharge dimensionless indexes ($\frac{Q_o}{\sqrt{g}D_o^5}$) for different sediment height dimensionless indexes ($\frac{H_s}{D_o}$) (a) and different angles between the branches (θ) (b).

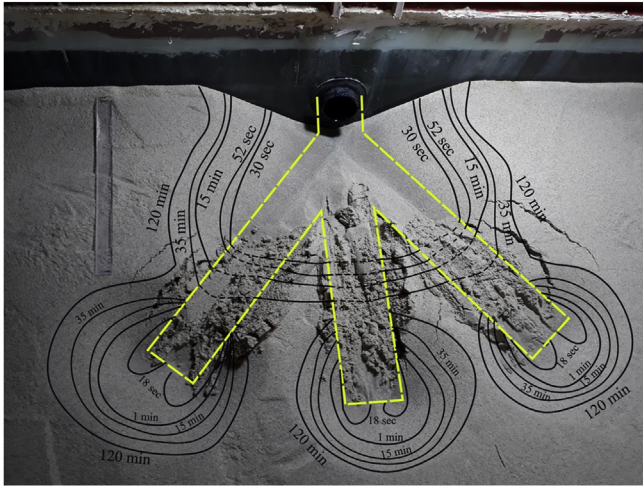


Fig. 13. Temporal development of the sediment flushing cone, $a_{3,3}$ configuration (Table 1).

the reference value, the maximum increase in the width of the sediment flushing cone is equal to 1.47 times the reference value, and the depth of the cone with a constant increase is equal to 1.2 times the reference test value for the three levels of blockage. These findings are identical to the results of Madadi et al. (2017).

Equations (5)–(7) present the relations between the sediment flushing cone dimensionless indexes and the relative sediment levels, outlet discharges, and angles between the branches (the main variables in Eq. (4)), consisting of the sediment head dimensionless index above the reservoir bed for $3.59 \leq \frac{H_s}{D_o} \leq 4.59$, the outflow discharge dimensionless index for $0.99 \leq \frac{Q_o}{\sqrt{g D_o^5}} \leq 1.43$, and the angle between the branches for $30^\circ \leq \theta \leq 60^\circ$.

$$\frac{L_c}{D_o} = 236.563 \left(\frac{H_s}{D_o} \right)^{0.069} + 232.256 \left(\frac{Q_o}{\sqrt{g D_o^5}} \right)^{0.04} - 487.479 (\sin \theta)^{0.003}, \quad R^2 = 0.827 \quad (5)$$

$$\frac{W_c}{D_o} = 0.064 \left(\frac{H_s}{D_o} \right)^{3.068} \left(\frac{Q_o}{\sqrt{g D_o^5}} \right)^{0.514} (\sin \theta)^{-0.069}, \quad R^2 = 0.91 \quad (6)$$

$$\frac{D_c}{D_o} = 0.006 \left(\frac{H_s}{D_o} \right)^{3.73} \left(\frac{Q_o}{\sqrt{g D_o^5}} \right)^{0.048} (\sin \theta)^{-0.102}, \quad R^2 = 0.997 \quad (7)$$

Fig. 9 shows the observed dimensionless values of L_c , W_c , and D_c against the values calculated using Eqs. (5)–(7), respectively. According to results and the standard error (SE) lines representing the average distance the observed values fall from the regression line, the regression lines for length, width, and depth dimensionless indexes fell between $\pm 5\%$ SE lines, indicating suitable agreement between the observed and calculated values.

The sediment flushing cone cross-sectional data can be used to investigate the structure's operation. The transverse cross sections of the sediment flushing cone in tests $a_{3,3}$, $b_{3,3}$, $c_{3,3}$, $d_{3,3}$, and $e_{3,3}$ for

three different distances of $Y/D_o = 0.5$, $Y/D_o = 1$ and $Y/D_o = 6.36$ according to the coordinate system of the experimental setup (Fig. 10) are shown in Fig. 11. According to the figures, the dimensions of the sediment flushing cone decreased with increasing distance from the outlet, which is consistent with the results of Madadi et al. (2016). The results indicate that the sediment flushing cone in test $a_{3,3}$ has the maximum dimensions in comparison with the other tests because of the limited flow; notably, the branches intersect each other at one point and create strong wake vortices.

Based on the gathered experimental data the best structural effect on the sediment flushing cone dimensions is the operation of the DBE structure with a 30° angle between the branches compared to the PSC structure and the other DBE structures with different angles between the branches. The other DBE structures with 45° and 60° had lower ranks, indicating that the lower the angle of the branches to the outlet current axis is, the stronger the shear force of the vortices and the greater the evacuation of sediment.

The interrelation between the limit distances of scour from the outlet and outlet discharge shown in Fig. 12a for different sediment height dimensionless indexes and Fig. 12b for different angles between the branches.

It can be seen that the distances of scour from the outlet increase as the sediment height increases, the structure's angle between branches decreases, and the outlet discharge increases. The diagram indicates that the best operation of the DBE structure is for the sedimentary dimensionless index of $H_s/D_o = 4.59$ and the flow dimensionless index of $Q_o/\sqrt{g D_o^5} = 1.43$ with a 30° angle between the branches (i.e., $a_{3,3}$ configuration).

The scour cone geometry strongly depends on the friction angle of the sediment (Fathi-Moghadam et al., 2010). In the current research, the side slope angle of the scour cone is approximately close to the submerged friction angle of the sediment, 29° , which is in agreement with the results of other studies for non-cohesive sediment (Fathi-Moghadam et al., 2010; Madadi et al., 2017).

3.2. Temporal development of sediment flushing cone

The tests were continued until the variation in the dimensions of the sediment flushing cone was negligible. The time duration of the scour balance was approximately 240 min. Sediment cone development immediately starts after opening the low-level outlet valve because a high turbulent flow creates and leads to the formation of the sediment flushing cone. This process decreased with time, and approximately 85%–90% of the scouring process occurred in the first 15–20 min after the start of each experiment. Finally, after approximately 120 min, the shape variation of the sediment flushing cone stopped. The temporal development of the sediment flushing cone is shown in Fig. 13.

3.3. Investigation of the volume of the sediment flushing cone

In this regard, the largest volume was due to the state with a 30° angle between the branches with a sedimentary dimensionless index of $H_s/D_o = 4.59$ and a dimensionless index of flow of $Q_o/\sqrt{g D_o^5} = 1.43$ and was equal to 0.0764 m^3 ; this is an increase of 10 times compared to the reference test and an increase of 2, 1.754, and 1.433 times compared to the PSC, DBE 60° and DBE 45° , respectively, for identical conditions. The 3D maps of the mentioned tests are shown in Fig. 14.

Based on the experimental results, Eq. (8) represents the relation for the sediment flushing cone dimensionless index and the main variables in Eq. (8) consist of the sediment head above the

reservoir bed, the outflow discharge and the angle between the branches with the same constraints as for Eqs. (5)–(7).

$$\frac{V_c}{D_o^3} = 1.981 \left(\frac{H_s}{D_o}\right)^{1.296} \left(\frac{Q_o}{\sqrt{g D_o^5}}\right)^{1.767} (\sin \theta)^{-1.114}, \quad R^2 = 0.98 \quad (8)$$

Fig. 15 shows the observed values of the sediment flushing cone volume dimensionless index against the value calculated using Eq. (8). According to results and the standard error (SE) lines representing the average distance the observed values fall from the regression line, the regression line for the volume dimensionless

index fell between ± 5% SE lines, indicating suitable agreement between the observed and calculated values.

3.4. Sediment removal efficiency

The sediment removal efficiency is a measure of the success rate of sedimentation (Madadi et al., 2016). According to past field research, the efficiency of the under pressure flushing operation is very low, and a high volume of water should be removed from the reservoir of behind the dam so that a small amount of the accumulated sediment is transferred downstream (Emamgholizadeh et al., 2006).

The sediment flushing efficiency is defined as the ratio of the volume of the sediment to washed (flushed) away to the volume of

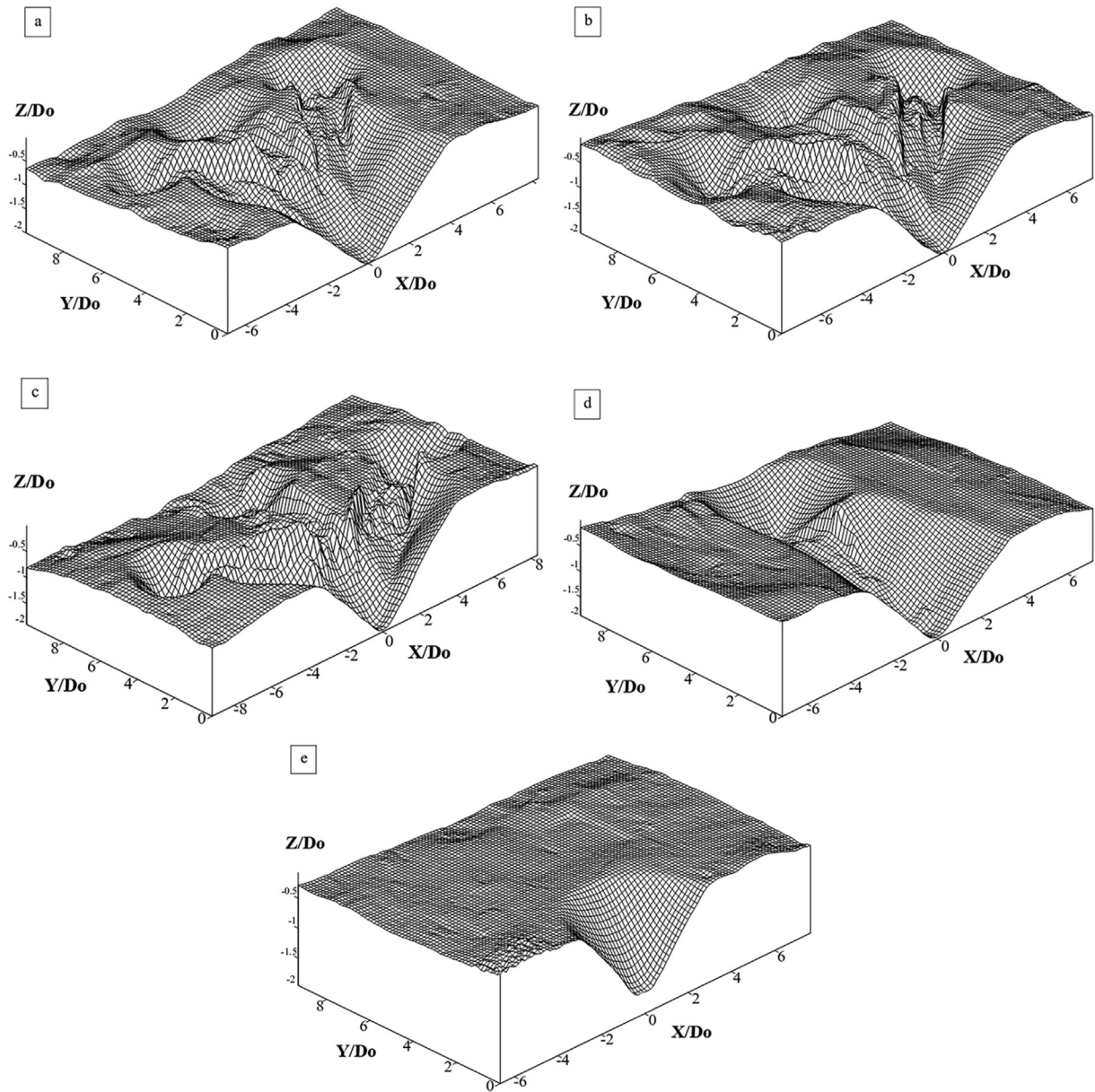


Fig. 14. 3D representation of flushing cones in front of the bottom outlet for DBE 30° (a_{3,3} configuration) (a), DBE 45° (b_{3,3} configuration) (b), DBE 60° (c_{3,3} configuration) (c), PSC (d_{3,3} configuration) (d), and the reference test (e_{3,3} configuration) (e) (Table 1).

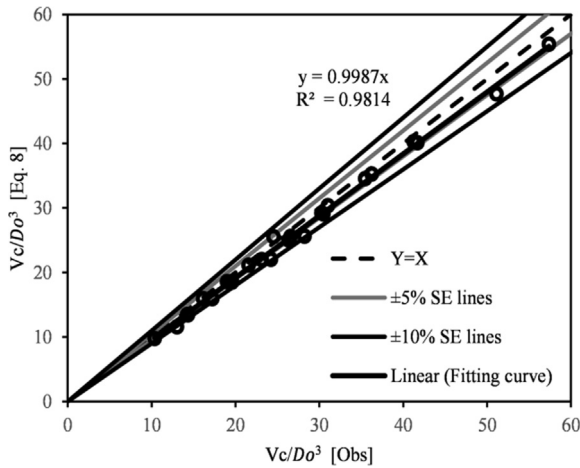


Fig. 15. Observed vs. calculated sediment flushing cone volume dimensionless index.

water used in the flushing. The sediment flushing efficiency is as follows:

$$E = \frac{V_c}{V_w} \tag{9}$$

where E is the flushing efficiency; V_c is the evacuated sediment volume from the reservoir during flushing (m^3); and V_w is the evacuated volume of water from the reservoir during flushing (m^3).

In the current study, the flushing efficiency was 0.1% in the $e_{3,3}$ configuration (reference test) and it was 0.498% in the $d_{3,3}$ configuration (PSC structure) for the sedimentary dimensionless index of $H_s/D_o = 4.59$ and a dimensionless index of flow of $Q_o/\sqrt{gD_o^5} = 1.43$. In the DBE structure with a 30° angle between the branches, for the sedimentary dimensionless index of $H_s/D_o = 4.59$ and a dimensionless index of flow of $Q_o/\sqrt{gD_o^5} = 1.43$, the flushing efficiency was equal to 1.01%, which indicates an increase of 10 times compared to the reference test ($e_{3,3}$ configuration) and 2.03 times compared to the value for the PSC structure test ($d_{3,3}$ configuration). In addition, the use of the other DBE structures with 45° and 60° caused increases of 6.98 and 5 times, respectively, compared to those in the reference test and 1.41 and 1.16 times, respectively, compared to those in the PSC structure test (Fig. 16).

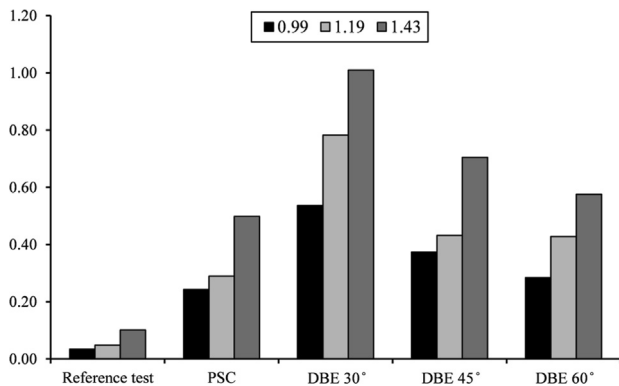


Fig. 16. Variation in the sediment removal (flushing) efficiency (%) for the sedimentary dimensionless index of $H_s/D_o = 4.59$ for different discharge dimensionless indexes according to the type of structure.

4. Conclusions

The structural effects on the sediment flushing cone dimensions using a new structure with branch angles of 30° , 45° , and 60° named DBE structures, were investigated and compared with those of a previous structure, PSC, and a reference test without any structure. The DBE structure should be considered in the design stage of the dam from the very beginning of dam construction. The experiments were done for three flows of 12.5, 15, and 18 L/s, and three sediment heights of 39.5 cm (no blockage), 45 cm (blockage height = $0.5D_o$), and 50.5 cm (blockage height = D_o). The current study focused on non-cohesive and coarse sediment due to the complexities and uncertainties involved in modeling of cohesive sediment and the results are only valid for non-cohesive sediment. Consequently, the results indicated that using a DBE structure with an angle of 30° between the branches, a sedimentary dimensionless index of $H_s/D_o = 4.59$, and a flow dimensionless index of $Q_o/\sqrt{gD_o^5} = 1.43$ led to an efficiency increase of 10 times compared to the reference test and 2.03 times compared to the PSC structure test. In addition, with the increase in the dimensionless index of flow from 0.99 to 1.43, the length of the maximum increase in the sediment flushing cone reached 4.92 times the reference value, the maximum increase in the width of the sediment flushing cone was equal to 1.34 times the reference value, and the depth of the cone with a constant increase was equal to 1.21 times the reference test value for the three levels of blockage. With the increase in the dimensionless index of the sediment height from 3.59 to 4.59, the length of the maximum increase in the sediment flushing cone reached 4 times the reference value, the maximum increase in the width of the sediment flushing cone was equal to 1.47 times the reference value, and the depth of the cone with a constant increase was equal to 1.2 times the reference test value for the three levels of blockage. Finally, according to a statistical analysis of the laboratory data, a dimensionless equation with $R^2 = 0.98$ for the prediction of the sediment flushing cone volume and dimensionless equation for the prediction of the sediment flushing cone length, width, and depth, for the application range of this study which consists of $3.59 \leq \frac{H_s}{D_o} \leq 4.59$, $0.99 \leq \frac{Q_o}{\sqrt{gD_o^5}} \leq 1.43$, and $30^\circ \leq \theta \leq 60^\circ$, are presented.

Declaration of competing interest

The authors declare that they have no known competing financial interests or personal relationships that could have appeared to influence the work reported in this paper.

Acknowledgments

This research was supported by the Kerman Regional Water Company under Grant 97/45.

Notation

- D_{10} Sediment particle diameter at which 10% of the sample is finer than this value (m)
- D_{16} Sediment particle diameter at which 16% of the sample is finer than this value (m)
- D_{30} Sediment particle diameter at which 30% of the sample is finer than this value (m)
- D_{50} Median size of sediment particles (m)
- D_{60} Sediment particle diameter at which 60% of the sample is finer than this value (m)
- D_{84} Sediment particle diameter at which 84% of the sample is finer than this value (m)

D_C	Depth of the sediment flushing cone (m)
D_{DBE}	Diameter of the DBE structure (m)
D_o	Diameter of the bottom-outlet (m)
DBE	Dendritic bottomless extended structure
E	Flushing efficiency (dimensionless)
Fr	Froude number (dimensionless)
g	Acceleration due to gravity (m/s^2)
G_s	Specific gravity of the sediment (dimensionless)
H_s	Sediment head above the bottom-outlet (m)
H_w	Total water head above the bottom-outlet (m)
L_C	Length of the sediment flushing cone (m)
L_{DBE}	Length of the branches of the DBE structure (m)
N	Number of branches of the DBE structure (dimensionless)
PST	The photo scan technique to obtain the topography of the sediment cone in each experiment
Q_o	Outlet discharge (m^3/s)
R^2	Coefficient of determination of the prediction equations
Re	Reynolds number (dimensionless)
SE	The standard error lines representing the average distance the observed values fall from the regression line
W_C	Width of the sediment flushing cone (m)
θ	Angle between the branches of the DBE structure (dimensionless)
θ_f	Internal friction angle of the sediment (dimensionless)
ρ_s	Sediment density (kg/m^3)
ρ_w	Fluid density (kg/m^3)
μ	Fluid dynamic viscosity ($kg/m.s$)
∇_c	Volume of the sediment flushing cone (m^3)
∇_w	Volume of the evacuated water (m^3)

References

- Ahadpour Dodaran, A., Park, S. K., Mardashti, A., & Noshadi, M. (2012). Investigation of dimension changes in under pressure hydraulic sediment flushing cavity of storage dams under effect of localized vibrations in sediment layers. *International Journal of Ocean Systems Engineering*, 2(2), 71–81.
- Amirsayafi, P. (2015). Measures for success in dam bottom outlet design. *GSTF Journal of Engineering Technology*, 3(3), 111–117.
- Annandale, G. W., Morris, G. L., & Karki, P. (2016). *Extending the life of reservoirs: Sustainable sediment management for dams and run-of-river hydropower*. Washington, DC: World Bank Group.
- Brandt, S. A., & Swening, J. (2000). Sedimentology and geomorphological effects of reservoir flushing: The Chachi reservoir, Costa Rica. *Geografiska Annular*, 81(A3), 391–407.
- Dargahi, B. (2012). Reservoir sedimentation. In L. Bengtsson, R. W. Herschy, & R. W. Fairbridge (Eds.), *Encyclopedia of lakes and reservoirs. Encyclopedia of earth sciences series* (pp. 628–649). Dordrecht: Springer.
- Di Silvio, G. (1990). Modeling desiltation of reservoirs by bottom-outlet flushing. In H. W. Shen (Ed.), *Movable bed physical models* (pp. 159–171). Dordrecht, The Netherlands: Kluwer Academic Publishers.
- Dreyer, S., & Basson, G. (2018). Investigation of the shape of low-level outlets at hydropower dams for local pressure flushing of sediments. In *International conference of sustainable dam Engineering in an ever-charging world* (Cape Town, South Africa)
- Dreyer, S. (2018). *Investigating the influence of low-level outlet shape on the scour cone formed during pressure flushing of sediments in hydropower plant reservoirs* (M.Sc. thesis). South Africa: Department of Civil Engineering, University of Stellenbosch.
- Emamgholizadeh, S., Bina, M., Fathi-Moghadam, M., & Ghomeshi, M. (2006). Investigation and evaluation of the pressure flushing through storage reservoir. *Journal of Engineering and Applied Sciences*, 1(4), 7–16.
- Emamgholizadeh, S., & Fathi-Moghadam, M. (2014). Pressure flushing of cohesive sediment in large dam reservoirs. *Journal of Hydraulic Engineering*, 19(4), 674–681.
- Fathi-Moghadam, M., Emamgholizadeh, S., Bina, M., & Ghomeshi, M. (2010). Physical modelling of pressure flushing for desilting of non-cohesive sediment. *Journal of Hydraulic Research*, 48(4), 509–514.
- Fruchard, F., & Camenen, B. (2012). Reservoir sedimentation: Different type of flushing—friendly flushing example of Genissiat Dam flushing. In *Proceedings, ICOLD international symposium on dams for a changing world. June 5, 2012. Japan: Kyoto*.
- Isaac, N., & Eldho, T. I. (2019). Sediment removal from run-of-the-river hydropower reservoirs by hydraulic flushing. *International Journal of River Basin Management*, 17(3), 389–402.
- Jenzer Althaus, J. M. I., De Cesare, G., & Schleiss, A. J. (2014). Sediment evacuation from reservoirs through intakes by jet-induced flow. *Journal of Hydraulic Engineering*, 141(2), [https://doi.org/10.1061/\(ASCE\)HY.1943-7900.0000970](https://doi.org/10.1061/(ASCE)HY.1943-7900.0000970)
- Madadi, M. R., Rahimpour, M., & Qaderi, K. (2016). Sediment flushing upstream of large orifices: An experimental study. *Flow Measurement and Instrumentation*, 52, 180–189.
- Madadi, M. R., Rahimpour, M., & Qaderi, K. (2017). Improving the pressurized flushing efficiency in reservoirs: An experimental study. *Water Resources Management*, 31(14), 4633–4647.
- Malavoi, J. R., & El Kadi Abderrezzak, K. (2019). *Reservoir sedimentation, dam safety and hydropower production: Hazards, risks and issues* (pp. 50–53). Hydrolink, IAHR publishing.
- Meshkati, M. E., Dehghani, A. A., Naser, G., Emamgholizadeh, S., & Mosaedi, A. (2009). Evolution of developing flushing cone during the pressurized flushing in reservoir storage. *World Academy of Science, Engineering and Technology*, 3, 10–27.
- Meshkati, M. E., Dehghani, A. A., Sumi, T., Mosaedi, A., & Meftah, H. M. (2010). Experimental investigation of pressure flushing technique in reservoir storages. *Water and Geoscience*, 54, 132–137.
- Morris, G. L., & Fan, J. (1998). *Reservoir sedimentation handbook: Design and management of dams, reservoirs, and watersheds for sustainable use (electronic version)*. New York: McGraw-Hill.
- Pitt, J. D., & Thompson, G. (1984). The impact of sediment on reservoir life. Challenges in African hydrology and water resources. In *Proceedings of the harare symposium. International association of hydrological sciences publication No. 144* (pp. 541–548).
- Powell, D. N. (2007). *Sediment transport upstream of orifice* (Doctoral Dissertation). Department of Civil Engineering, Clemson University, Clemson, SC, U.S.
- Qian, N. (1982). Reservoir sedimentation and slope stability; technical and environmental effects. In *Proceedings, 14th international congress on large dams* (pp. 639–690). May 3–7, 1982, (Rio de Janeiro, Brazil).
- Randle, T., ... (2019). Reservoir sediment management: Building a legacy of sustainable water storage reservoirs. In *National reservoir sedimentation and sustainability team white paper*. Retrieved from <https://www.sedhyd.org/reservoir-sedimentation/National%20Res%20Sed%20White%20Paper%202019-06-21.pdf>. (Accessed 12 June 2019).
- Sayah, S. M. (2015). *Design and erection of the 6 bottom outlets of Cerro del Aguila Dam for flood routing during construction and future sediment flushing*. Hydro 2015, October 26–28, 2015, (Bordeaux, France).
- Schleiss, A. J., Franca, M. J., Juez, C., & De Cesare, G. (2016). Reservoir sedimentation. *Journal of Hydraulic Research*, 54(6), 595–614.
- Shahirnia, M., Ayyoubzadeh, S., & Mohamad Vali Samani, J. (2014). Investigation on the effect of sediment level on pressurized flushing performance from reservoirs using physical model. *Journal of Hydraulics*, 9(1), 11–25. (In Persian)
- White, R. (2001). *Evacuation of sediments from reservoirs*. London: Thomas Telford Publishing.